Environment and Natural Resources Research; Vol. 8, No. 1; 2018
ISSN 1927-0488 E-ISSN 1927-0496
Published by Canadian Center of Science and Education

Observation and Characterization of the Thermoelectric Power Generation

A. J. Jin[1,2], Q. Li[1], D. Liu[1], C. An[2], Y. Zhang[2]

[1] Solar Thermal Energy Division, Hua-Neng Clean Energy Research Inst., 100 QiBei Road, Beijing, China

[2] Additive Manufacturing Division, Ningbo Institute of Industrial Tech, Chinese Academy of Sciences, 1219 Zhongguan W. Rd, Ningbo, China

Correspondence: A. J. Jin, Solar Thermal Energy Division, Hua-Neng Clean Energy Research Inst., 100 QiBei Road, Beijing, China. Tel: 86-186-0069-9878. E-mail: ajjin@hnceri.com

Received: December 27, 2017 Accepted: January 25, 2018 Online Published: February 26, 2018

doi:10.5539/enrr.v8n1p94 URL: https://doi.org/10.5539/enrr.v8n1p94

Abstract

Authors report methodical studies on some novel, alternative energy technologies, and produced results of a thermoelectric power generation (TEPG) system. For the sake of evaluating critical thermoelectric (TE) features, they have invented the state-of-the-art equipment that has important specification capability. The studies cover the efficiency and many aspects of TEPG features as follows. A thermoelectric module is measured in situ that includes TE efficiency, force response curve, current-voltage (I-V) and power-voltage (P-V) characterization, and power temperature (P-T) response curve. They have improved both the higher total output power and the more efficient TEPG efficiency than their comparison TE devices and systems in their studies. In addition, authors will present a series of design, construction, and characterization of a thermal electric generation system which aims to achieve a large power output and high efficiency for the energy harvesting application. Furthermore, their studies lead to important knowledge of TEPG systems in terms of multi-stack modules and of the optimization in TEPG applications. Finally, the prototypes are built for both the tabletop and other applications with new findings. Several sets of prototype TEPG are developed for experimental investigation and data analysis, followed by the summary and conclusions based on the data.

Keywords: thermoelectric, energy harvest, efficiency, in-situ

1. Introduction

In order to reduce the greenhouse gases emissions problem and to address the climate change issue, a huge cooperative effort has been achieved through the hallmark of the Paris Agreement (Agreement) (Note 1). The Agreement is also called Accord de Paris which is an agreement of member nations of the United Nations. By April 2017, 195 nations has signed on it; their cooperation is believed to be essential in the combat or control of the climate change in part. Extensive research and development has been dedicated to renewable energy (RE) technologies by scientific communities in order to advance RE (Brass et al., 2012). One of the key hallmarks in the Agreement is to significantly commercialize the technology in renewable energy production and to reduce the carbon emission from traditional fossil-based fuels.

The fossil fuel based energy is considered as an insecure energy source that causes power shortage, PM2.5 air pollution, and relevant geographic concerns or instability to name a few. Along with the outdated grid system, the traditional energy system is attributed to causing major electricity blackouts numerous times.

Therefore, there are tremendous interests in leading researchers to develop the distributed power generation (Brass et al., 2012; Clark, 2015; Chen, 2011; Deng & Liu, 2009) particularly with a renewable energy system in order to fix the above issues and to have more advantageous energy generation. To date, there have been curious debates on this policy in the world, which was demonstrated in the recent two administrations in the United States of America with an opposing position of the renewable energy emphasis.

Several alternative energy technologies have the clean technologies with commendable breakthroughs. A new technology breakthrough like many in the past can bring in new markets. The important application includes renewable and unique applications, such as Mars Rover (Tritt & Subramanian, 2006), with new energy sources. The technologies being successfully commercialized to date include the following: solar, the wind, solar thermal,

geothermal, thermo-electric, biofuel, and nuclear energy technology; other technologies to mitigate the clean energy shortage includes liquefied natural gas (LNG), hydrogen fuel, and petroleum fracking. Moreover, there are extensive works to extend clean technologies to the traditional fuels such as the cleaner coal technology for the sake of removing harmful emissions such as SO2, NOx, and carbon emission by-products. Both solar energy and wind power are among these widely commercially adopted with relatively mature technologies for energy systems in sustainable communities' designs (Clark, 2015).

So far, the solar technology is one of the most important RE technologies that has provided photovoltaic solar energy solutions in the United States. Some European countries have successfully employed the solar renewable electricity technologies. For example, Germany has achieved one-third of its national total energy shares with the renewable energy in the year 2016. Germany is generally regarded as being a successful leader in the solar tariff, followed by Japan that has significant installed solar-power capacity. The solar users are vastly distributed in the developed nations with an exception that China is currently attaining the largest photovoltaic market on the installed basis in the world. Finally, the Chinese companies have produced PV in volume and top-ranked panel makers that enabled the progress toward the grid parity.

Distributed Power Generation (DPG) produces electricity at or near the point where it is used with the suitable amount of electricity. DPG is equipped with some sensors connected to the computers which can relieve the burdens of utility systems due to the increase in reliability for interconnecting control in the power usage (Clark, 2015).

There has been extensive research recently dedicated to studying the thermoelectric power generation (TEPG) in producing power ranges from small to large. In contrast to the solar technology that has solar panels, it collects photon energy and converts it into electricity, a very different type of RE is the TEPG technology that directly makes energy conversion from heat into electricity. This conversion follows a law of physics called Seebeck effect (Thomson, 1857). TEPG with the thermoelectric modules (TEM) generates energy from natural heat sources such as solar, geothermal, and afire source, and other heat sources like waste heat/ energy harvesting. The thermoelectric energy is advantageous as the RE in many ways, including that it has no carbon emission in part, and its noiseless with no moving parts, light weight, no need or little need for maintenance.

TEM is made of TE materials and is usually a solid-state device. The device integrates a large number of pairs that are typically semiconductors thermoelectric, that convert heat directly into electricity, and that each pair contributes typically hundreds of microvolts per degree of temperature difference. When located in either the hot or the cold environment compared to the ambient, a TE device produces a small voltage and thus generate electrical power when they connect to a resistive load. A large number of devices can enable TEM to provide a large power output (Jin et al., 2013). The TE energy conversion field is of tremendous interests and has attracted huge amount of studies on topics such as the conversion from various thermal energy into electricity (Yang & Yin, 2011; Min, & Rowe, 2017).

More recently, the TEPG technology has been extensively explored in applications. Researchers have investigated TEPG with natural heat sources and waste heat that achieves technology breakthroughs in terms of both improved thermal electric efficiency and large power output. One of the most important factors is ZT a.k.a. the figure of merit of a TE material. The TE law of physics can be understood by a simplified illustration as follows. For a single TE mat'l, its capability related to TE conversion can be described by ZT.

$$ZT = \frac{S^2 T}{\rho k} \tag{1}$$

Where S is a TEM Seebeck coefficient of the material, T is its temperature, ρ is its electrical resistivity, and κits thermal resistivity.

The physical TE effect obeys the Seebeck effect that converts thermal energy directly into electrical energy; a device often has two dissimilar TE materials.

The TE junction of a pair of TE materials has a combined figure of merit. As mentioned before, a device typically requires a pair of N-type and P-type dissimilar materials to form TE junctions. The combined figure of merit $Z_{NP}T$ [ZT] is at below.

$$ZT = \frac{(S_P - S_N)^2 T}{[(\rho_N k_N)^{1/2} + (\rho_P k_P)^{1/2}]^2} \tag{2}$$

where S_P and S_N is the Seebeck coefficient of P-type and N-type, respectively. ρ_P and ρ_N is the electrical resistivity of P-type and N-type, respectively. κ_P and κ_N is a thermal resistivity of P-type and N-type, respectively.

The output voltage ΔV increases with and has basically a linear dependence upon the temperature differential ΔT. For a combination of N-type and P-type materials, ΔV is given at below.

$$\Delta V = S_{NP} * \Delta T \tag{3}$$

The constant S_{NP} equals to S_P - S_N and is called a Seebeck coefficient of the TE pair. The constant is related to pairs of materials properties (Tritt, & Subramanian, 2006; Thomson, 1857). It is clearly demonstrated at above that ZT succinctly relates to the TE-efficiency, η, in a mathematical formulae at below. The efficiency is the ratio of power generation W to the heat input of a system Q_h. Therefore, the goal to increase TE efficiency is to improve the material's ZT. The math relationship is shown as follows.

$$\eta = \frac{W}{Q_h} = \frac{T_h - T_c}{T_h} * \left[\frac{(1+ZT_m)^{1/2} - 1}{(1+ZT_m)^{1/2} + (T_c / T_h)} \right] \tag{4}$$

where T_h, T_c and T_m are its temperatures at the hot side, cold side and average of both hot and cold sides of the TE device. ZT_m is its figure of merit at its average temperature.

It is imperative for the TEM to improve its efficiency, and highly desirable to attain large TEM output power so that it is significant and viable for successful commercial applications. If the TEM technology is to be commercially successful, one significant factor is that the efficiency should achieve some system level, for example, that ZT >= 2. When the TEM be commercialized, the applications are very significant which include part of the power generation, usable electric energy to power small electronic devices, and recycle and reuse the energy which otherwise would be wasted.

ZT may characterize the performance of thermoelectric materials which includes parameters such as the Seebeck coefficient (S_{NP}), thermal conductivity, and electrical resistivity (Mao, Liu, & Ren, 2016; Liu et al., 2015; Nolas, Sharp, & Goldsmid, 2013). The TE properties of most semiconductors depend upon temperature, e.g., a single TE material typically operates in about 200 K temperature window (Crane et al., 2009).

Finally, this article is presented as follows. Authors have conducted extensive studies and a variety of experiments; important findings are reported in the article. In this section, they provide a brief introductory background of the alternative energy technology with an emphasis on TE and its applications. The next section describes the experimental setup and presents the TE results from the studies. In addition, it discusses the typical trends of these results. Furthermore, it will provide further analysis of these experiments and more discussion on the thermoelectric technology study that covers the TE devices advanced manufacturing technologies. Lastly, they present conclusion and summarize their important findings.

2. Experimental

This section will deliver systematic studies and cover the TE features and instrumental studies related to the TE devices, module, and systems.

A. General TE instruments

A typical TE generator setup is shown in Figure 1 in order to illustrate an experimental system. This setup includes multiple system hierarchy of a TEPG. Based on laws of physics governing thermoelectric phenomenon, a typical TE device consists of two dissimilar TE materials. As heat flows across the temperatures of the T_h and T_c with a different delta-T that is illustrated in Figure 1a). The ΔT produces the electromotive force [emf] and causes the charge's motion as shown in the figure.

A thermoelectric module (TEM) is typically built with a large number of TE devices. A typical TEM is illustrated with a schematic shown in Figure 1b). Moreover, the prototype of TEPG is schematically shown in Figure 1c). At a dial-setting of LNG level when the ΔT reaches 200°C; the total power output is at a hundred watt level.

Figure 1a) shows that the heat flows through the temperature difference across a TE device that is composed of two dissimilar TE legs and that an electric flow is built up across the TE legs. Moreover, Figure 1b) shows a typical TEM that integrates a large number of TE devices for a power generation type; Figure 1c) is an actual TE power system where the TEPG is supplied by the LNG-burner heat source and produce a typical electric power at a hundred watt level.

A variation of the system depends on technology applications. When TEPG is built, researchers have applied careful thermal management methods and built systems at various power levels. The methods include the fine

insulation method, that will be described a bit later, and good uniformity conducting heat for both cooling surface and heating surface. In a normal system, the hot side employs one of the heating choices. That includes the infrared heat sources, LNG as for house heating and cooking fire, power heaters, or solar thermal and/or other methods. Make a note that the LNG is normally warmed to make natural gas for use in heating and cooking as well as electricity generation and other industrial uses. The above choices are laid to establish the groundwork of prototypes for various potential applications.

A TEG system is illustrated at below. A typical system shown in Figure 1 has operated on both an LNG burner and tap water [below 8 C for cooling in the lab. The output has reached a hundred watt level in power output.

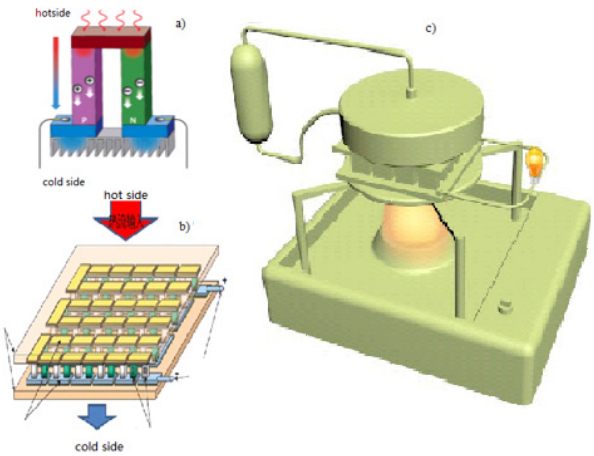

Figure 1. The schematics illustrates an operating principle of a TEPG as follows: 1a) schematic of a TE device composed of P- and N-type TE legs; 1b) a typical TEM integrates a large number of TE devices; 1c) a TEPG on both an LNG burner heating and tap water cooling [below at low temperature] that provides output power at a 100-Watt level

B. In-situ characterization

One of the examples in this article studies the characterization of an individual TEM. The in-situ characterization station for TEM (ICSTEM) is built on a house as shown in Figure 2. It shows the instrument design to measure the in-situ conversion efficiency of TEM among other applications. The ICSTEM instrument can measure the following variables: output power P, current I, voltage V, inner resistance R, and heat flux Q_c at the cold-end of the TEM under power generation state. As a result, ICSTEM can study the following TEM properties: 1) in-situ TEM efficiency; 2) I-V curve; 3) P-V curve; 4) force factor response.

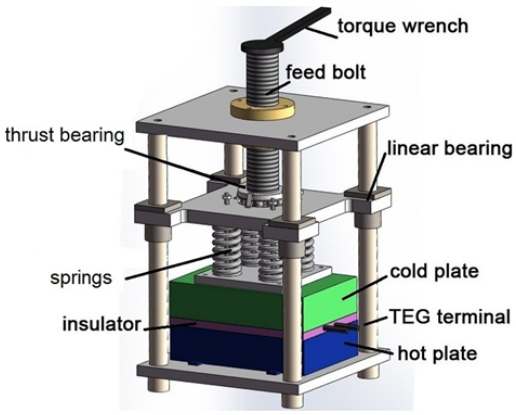

Figure 2. the ICSTEM instrument can set precise parallelism between the upper surface (cold plate) and the lower surface (hot plate). The temperature settings can be precisely controlled. In-situ characterization station can study the following TEM properties: 1) In-situ TEM efficiency; 2) I-V curve; 3) P-V curve; 4) force factor response. Details see text

The hardware configuration can direct the heat flow essentially along the z-axis. The efficiency is defined as the ratio of the electric power output to the heat input in the hot side of the TE device.

The force is set by a torque wrench through feed bolt. Both the springs and set screws enable separation in z-direction to achieve a fine resolution (about 5 microns) between the hot plate and the cold plate. By setting the cold plate at 25 °C which is achieved through the liquid nitrogen coolant control, the hot side can achieve above 450 °C per heater setting. This table top equipment has a wide range of temperature operation window.

As mentioned at above, the ICSTEM instrument is carefully designed so that the physics of heat flow can be well-described by that the heat flux flows along z-axis and that the thermoelectric conversion efficiency can be measured conveniently in-situ in real time. Theoretically, the cooling capacity Q_c is calculated as follows:

$$Q_c = S_{,PN}\, T_c\, I - \frac{1}{2} I^2\ R - k\,(T_h - T_c) \tag{5}$$

where S_{PN} is the TEM Seebeck coefficient, T_h is its temperature at hot-side, T_c its temperatures at cold-site, I current, R resistance, and k thermal resistance. The maximum cooling capacity is reached when the TEM has the same temperature at cold-side and at hot-side.

When the ICSTEM is designed, TEM should be placed flatly and be parallel with the two relative edges of the heat flux sensors near its cold-side. The heat insulation is carefully constructed with alternating multilayers made of pairs of the thin composite material of metal foils and fiberglass sheets. Its alternating layers of the thermal insulation are estimated to be far better [by a factor of tentimes or more effective] than the air would. The insulation layers range from a dozen pair to twenty pairs and work better than the asbestos material; the reasons are as follow. On one hand, the metal foil has high infrared reflection, according to calculations, multiple layers can reduce the influence of infrared radiation heat leakage to negligible extent; on the other hand, fiber-glass has low thermal conductivity with some air in the interval, which can significantly reduce the influence of the heat leakage and reduce the influence of the infrared radiation heat leakage to a negligible level.

The system is a tabletop instrument with small size. The system is thermally insulated at peripheral surfaces and has good uniformity conducting heat at both cool surface and heat surface. The hot-side controls temperature T_h with a specific heat source. The cold-side controls temperature T_c of the thermoelectric module under cooling conditions. In this case, the cold side employs one of the cooling choices [tap water, or liquid nitrogen cooled]. High infrared reflection and insulation materials, for example, may be chosen as the alternating layers of aluminum foil or thin metal sheet, and thin glass fiber sheet or insulator layer.

The thermal management utilizes the best available insulation by employing either the asbestos sometimes or many alternating layers of thin metal foils with glass fiber sheets that can cut down any significant heat loss.

This can significantly reduce the influence of the most heat leakage lost in heat conduction. The in-situ characterization station is carefully designed so that the physics of heat flow can be described well by the heat flux flows through the z-direction as the 1D heat flow (Liu & Jin, 2015). The model provides one of the best design parameters for TEPG designs. As the output power is measured, the total heat flux is known; therefore, the TE efficiency is their ratio that is readily derived. Simple computation based upon eq.1 derives the efficiency of a TE device.

C. Develop an energy harvest TEPG system

The other example in this article studies a design and a test of an energy harvesting TEPG at below.

The computer simulation is employed to aid the TEPG system design and its methodology is shown by a flow chart shown in Figure 3. Authors employ a design rule to achieve an optimized and a high-power TEPG output. A simulation algorithm is set up by utilizing the heat transfer model and by a finite element analysis for attaining an optimized system. A lab system is generally designed to deliver required voltage and provide output power to meet requirement.

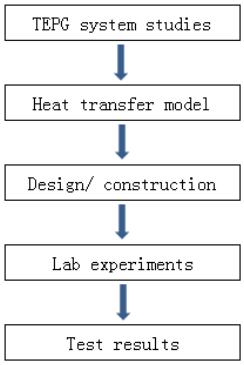

Figure 3. The flow chart illustrates a methodology to design, develop, and test the TEPG system. A goal is to maximize the total power output; the design employs a computer simulation about the related heat transfer model

Based on the above methodology, researchers have designed and constructed a prototype for the applications of automotive tail-pipe energy harvest [ATEH] unit. The ATEH has a sandwiched design with double layers of the TE generation that each layer contains dozens of TE modules. The ATEH includes an integrated assembly as shown in Figure 4a) that has been installed to introduce both the hot gas flow and the cooling media in the TEPG.

Referring to Figure 4b), dozens of TE modules are arranged with a designated circuitry configuration in order to meet the required output specification. Figure 4a) illustrates the sandwiched ATEH unit components. As shown in Figure 4c), the heat flows from the left side, and the cooling is supplied that is located at its top, bottom, and sandwiched layers in the middle-center. The heat flows into the ATEH from the left side hinge and out from the right.

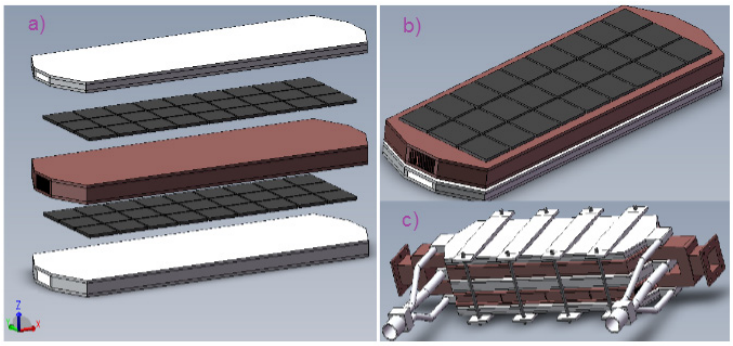

Figure 4. The energy harvest device illustrates an integrated assembly as follows: a) dual stack in sandwich structure; b) a batch of TEMs configuration; c) energy harvest unit that hot gas heat flows in from the left side hinge and out from the right

3. Results and Discussion

The authors have explored a whole range of TE features that are reported in successive sub-sections.

3.1 Data and Analysis

Several methods of measurement are employed. Researchers build several TEPG for high-tech applications. They have investigated approaches in order to improve both the thermoelectric efficiency and the desired output at the higher system levels.

The TEPG system has a relatively small size that is thermally insulated at peripheral surfaces and has good uniformity conducting heat for both the cold surface and hot surface. A number of heat sources and/or cooling mechanism are employed to a good extent of success to demonstrate a range of TEPG power output. Several heater options are investigated as follows: the infrared heater is used as a heat source, the direct-fired diesel burner employed, or the LNG burner employed as well.

The samples of TEM include off-the-shelf devices (Solla, 1981) and home-built devices. The thermoelectric devices have employed TEMs with both in-house built and off the shelf devices (Jin et al., 2013; Liu et al., 2015).

The hot side controls the temperature T_h with any given heat source; the cold side controls the temperature T_c of the thermoelectric module under cooling conditions. In this case, the cold side employs one of cooling choices [e.g., water or liquid nitrogen cooled]. High infrared reflection and insulation materials, for example, may be chosen as the alternating layers for thin metal sheet and thin glass fiber sheet [or insulator layer]. This can significantly reduce the influence of the heat leakage in heat conduction. The in-situ characterization station is carefully designed so that the physics of the heat flow can be well described by a 1D heat flow model (Liu & Jin, 2015) and that the heat flux simply flows along z axis. This example, which is based on the 1D model, is studied experimentally; the test data is in a good agreement as it will be discussed later.

As shown in Figure 5a) and b), a TEM device (Note 2) is selected among many options and characterized for its fundamental electrical property traces in terms of current (I, in unit of Ampere) versus voltage (V, volt) curves, i.e., I-V curves, and in terms of power output [at maximum value point] (P, Watt) versus V, i.e., P-V curves.

The figures have plotted typical data of a system at three different temperature settings. Figure 5a) shows I-V curves exhibiting typical electrical traces of a low resistance power supply; and Figure 5b) shows P-V relationship. The curves trace a typical behavior of the resistive power output; the power output increases with temperature T_h.

Researchers discover a relationship of TEM output power and the applied clamping force shown in Figure 5c). At the low force region, the power increases significantly with the force. The curve exhibits a total variation of twenty percent that is often observed in various temperature settings. The module performance curve is typically dependent upon its surface force a.k.a. pressure. As it is shown, a force chosen at 125kg to 250kg works well where the curve essentially flattens. This study chooses 250kg in the force setting.

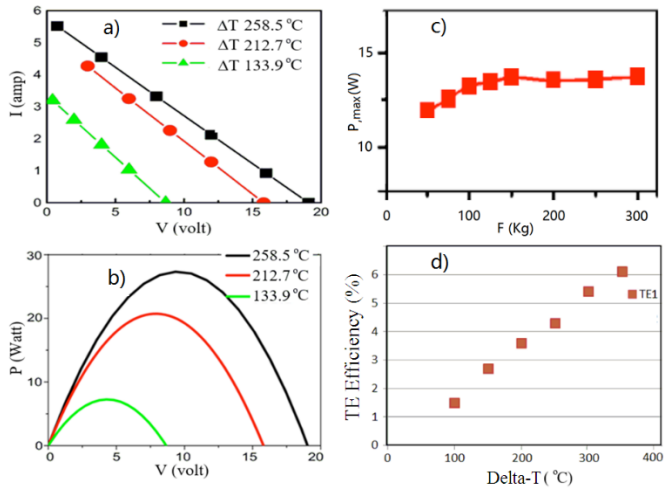

Figure 5. the data are illustrated as follows: a) I-V curve; b) P-V curve. Both I-V and P-V curve are shown in a module with T_c at 25 °C, T_h shown in figure. c) The TE power output depends on the surface clamping F as shown; d) the TE efficiency shows dependence upon the temperature differential

A typical force response curve is shown in Figure 5c). The variation in the pressure range is most likely due to reasons of contact voids, electrical contact resistance, and any air gap within the TE module and interfacial structures. The afore-mentioned defects may be caused by packaging materials and the related circuitry of TE devices. The aforementioned defect or imperfection [of TEM] can be optimized through proper setting of the clamping force. The optimization may reduce extra parasitic losses with optimized setting with low parasitic losses: e.g., low contact resistance, small radiation effects, little inter-diffusion at any junction.

The TE energy conversion efficiency is measured that depends upon the operating temperature as it is shown in Figure 5d).

3.2 Energy Harvest Studies

As shown in the prior section, the flow chart in Figure 13 illustrates a current research and a methodical approach through the design, construction and testing for a TEPG system. The system aims to produce an optimized large

output and is carefully executed based on the finite element analysis and the heat transfer model of the SolidWorks® (Note 3).

Authors have constructed a prototype for the applications of automotive tail-pipe energy harvest (ATEH). The ATEH has the sandwiched design with double layers of the TE generation that each layer contains dozens of TE modules. Based on the combined multiple-unit studies, the total power output is superimposed well in either serial or parallel configuration and typically equals to a sum of all units of individual TEPG (Jin et al., 2013). The ATEH is an integrated assembly that is installed to introduce both a hot gas flows through and a cooling media in TEPG.

Referring to Figure 4b), dozens of TE modules are arranged with a desired circuitry and/or configuration in order to meet the required output specification. Figure 4a) illustrates the sandwiched ATEH hardware components. As shown in Figure 4c), the heat flows from the left side, and the cooling is supplied that is located at its top, bottom, and two sandwiched layers in the middles and at the center.

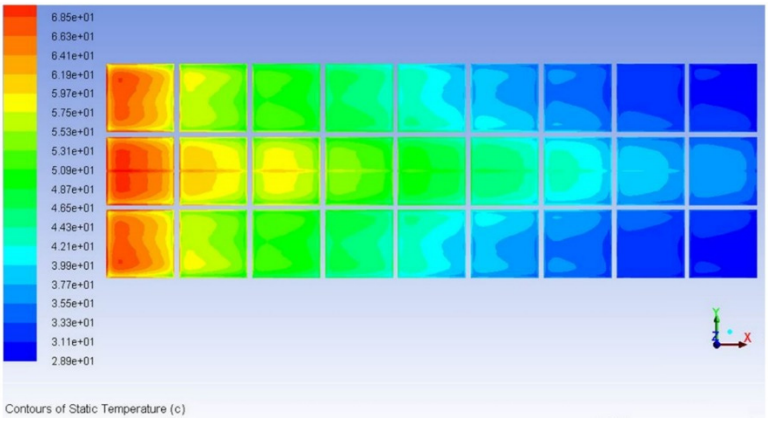

Figure 6. The temperature [T] distribution is derived from the computer simulation. A typical T-distribution is shown across the XY plane. Along X-axis, T decreases corresponding to the down-stream of heat flow. Along the Y-axis, T has small variation showing a center-to-edge variation

As an instance, the design model has delivered a typical temperature variation across the XY plane which is shown in Figure 6. The temperature variation is as expected due to the conditions that the viscosity of the hot gas is higher near the edge of the prototype than near the center and that the gas near the edge is cooler. The temperature near the center should be higher across the Y-direction.

The P-vs-T curve is measured in the laboratory tests as shown in Figure 7. Various prototypes are built and tested. Based on the tests of the TEPG system (ATEH system), the total output power reaches 1kW (1080W at 315 °C).

In addition to the above laboratory tests, a prototype is successfully applied and is installed on a pickup car for the road tests. The tests exhibit significant improvement of the gasoline mileage for a side to side comparison either with ATEH or without ATEH configuration; the road test covers a thousand kilometers for each compared configuration.

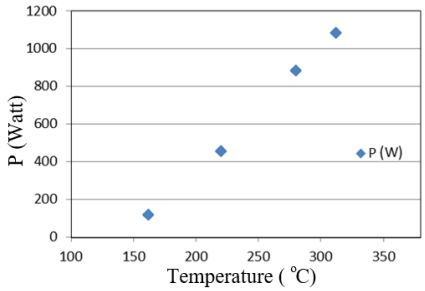

Figure 7. Lab tests for the power output of a TEPG shows that its maximum output depends linearly on the temperature in the tested range

3.3 Multi-stack TEG Data

A desirable high performance system is imperative for a wide application of its related high tech of TEPG; the technology requires an advanced manufacturing method and achieves a high energy efficiency than TE devices are currently in the market. The reason is that the existing materials have a relatively small operation window in temperature, and the efficiency is relatively small. In the current situation, it is common that ZT is not high enough, and the optimum operational window for ZT is less than two hundred degrees.

The system can be improved as follows. As shown in Figure 8, the multi-stack structures of the TE devices are studied in order to enhance ZT and to achieve a large TE efficiency. There are advanced technologies going on for the new production method.

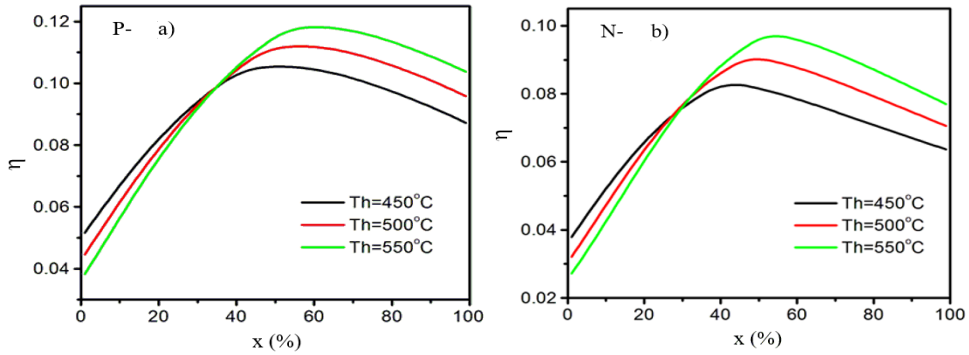

Figure 8. the dual-stack TE devices are illustrated for both P-type and N-type materials at below: 8a) the P-type efficiency shows dependence upon x; 8b) the N-type depends on x. The temperature is chosen at three different settings as illustrated. Individual TE property refers to the Table-I

A number of experiments and computer modeling works are conducted on multi-stack structures. By choosing the TE materials available in the market, the multi-stack TE materials selected have commensurate temperature and the TE device can increase the operating temperature window. As a result, the selection of TE materials is shown in Table I, and the dual-stack achieved an efficiency of 10.07% for dual-stack that is far greater than the single stack BiTe efficiency.

Figure 8 illustrates the dependence of efficiency upon the length ratio (x) for both the P-type and N-type TE materials, where x is the joint position in the ratio of the length where segmented legs are located. Figure 8a) shows the P-type efficiency as a function of x at three temperature settings; Figure 8b) shows N-type as a function of x. The TE efficiency is 11.8% at 550 °C of T_h for the P-type, and it is 9.7% at 550 °C for N-type on the hot side. Note that the variable x is the location ratio along the segment of each dual-stack TE leg.

As it is shown in the Table I, the dual-stack materials consist of the Pb-Te based and Bi-Te based TE materials. The Pb-Te based materials [and its variation stoichiometry] include both in P-type and in N-type TE materials optimized for a medium-temperature range. The Bi-Te TE materials [and its variation stoichiometry] includes both in P-type and in N-type TE materials optimized for a low-temperature range. The dual-stack of both P- and N-type PbTe on BiTe based segmented-legs are joined together through hard soldering at high temperature that cannot otherwise be welded together. A dual stack TE system exhibits the enhancement of the figure of merit, ZT. The ZT values are tabulated for several TE materials covering high-temperature [windows] in Table I at below.

Table I. the figure of merit ZT is illustrated as a function of temperature at below. (P-PbTe: $Pb_{0.94}Sr_{0.04}Na_{0.02}Te$, N-PbTe: $Pb_{0.94}Ag_{0.01}\,La_{0.05}Te$, P-BiTe: $Bi_{0.5}Sb_{1.5}Te_3$, N-BiTe: Bi_2Te_3)

P- PbTe		N- PbTe		P- BiTe		N- BiTe	
T(K)	*ZT*	T(K)	*ZT*	T(K)	*ZT*	T(K)	*ZT*
321	0.17	320	0.18	327	0.88	326	0.83
422	0.48	420	0.39	379	0.95	373	0.94
522	1.13	524	0.71	431	0.91	423	1.11
622	1.76	620	1.09	482	0.72	524	0.92
722	1.86	726	1.44				
822	2.12	824	1.51				
922	2.05	924	1.41				

The manufactured devices are composed of BiTe/ BiSbTe based and PbTe-based [TE, Table I] thermoelectric materials. The measurement efficiency is measured. The measured data, and simple computation based upon eq.(5) derives the efficiency.

Authors have explored various materials, investigated many system setups, and surveyed through a wide range of temperature difference. A research is conducted on related manufacturing approaches so that one can attain a higher temperature difference, more energy density, and better output performance in terms of the TE efficiency than what is currently available (Jin & Zhang, 2017).

The multi-stack TEG system is advantageous in the output system efficiency. By comparing the curve-A [close-system], and curve-B [open-air], it is apparent that the enhanced system thermal management has significantly improved the output efficiency. If the unit cost continues to drop from the current price of the off-the-shelf TEM, and theoretically, if ZT =~ 2.0, the TEPG can possibly achieve a large scale by economic value added (Jin & Zhang, 2017).

ZT is related to the material properties including the electrical conductivity, thermal conductivity, and the Seebeck coefficient. The ZT of the employed TE materials for segmented legs is listed for the related TE materials in Table I. The favorable working temperature of PbTe based materials used for the high-temperature segment was from 573 K to 873 K, and the dimensionless figure of merit in this temperature range ($ZT = S^2/\rho\kappa$) was about 1.5~2.1 for the P-type and 0.9~1.4 for the N-type. The favorable working temperature of BiTe based materials used for the lower temperature segment was from room temperature to 573 K; the dimensionless figure of merit in this temperature range was about 0.7~0.9 for P-type and 0.8~1.1 for the N-type. The improvement efforts of ZT in the thermoelectric materials have attracted extensive studies (Mao, Liu, & Ren, 2016).

4. Conclusion

In summary, researchers has built and studied several TEPG devices, modules, and systems. This research has succeeded in improving both the output level of TEPG and its efficiency. By utilizing commercially available TE materials, the dual stack TE device has achieved over 10% efficiency experimentally in this study; the triple stack TE device has resulted in 19% efficiency based on the computer modeling with available TE materials. Moreover, an instrument of in situ characterization is for the studies of the TE efficiency, I-V curve, and P-V curve over a wide temperature window. Finally, researchers have demonstrated at 1kW and above in output of a TEPG system prototype. The experiments have methodically presented the performance data for various thermoelectric systems.

Acknowledgments

This work is funded in part by the Beijing Science and Technology Foundation for the clean air projects, and for the research and application of thermoelectric technology, under grant TW12BJKW01. A.J. thanks the China Hua Neng Group for its reasearch grant provision for special oversea returnees.

Notes

Note 1. Paris Agreement. (2018). The Paris Agreement deals with greenhouse gases emissions mitigation, adaptation and finance starting in the year 2020. By April 2017, 195 nations of the UN member nations have signed on the Agreement, 145 of which have ratified it. In *Wikipedia, the free encyclopedia*. Retrieved from https://en.wikipedia.org/wiki/Paris_Agreement

Note 2. One of the commercial TEMs is employed for reference in part, for example, TEM No. TEHP1-12656-0.3 from the manufacturer owned by Thermonamics Electronics Corp., Ltd., China.

Note 3. SolidWorks is a solid modeling computer-aided design (CAD) and computer-aided engineering (CAE) computer program. SolidWorks Copyright is owned by SOLIDWORKS Corp, USA.

References

Brass, J. N., Carley, S., MacLean, L. M., & Baldwin, E. (2012). Power for development: A review of distributed generation projects in the developing world. *Annual Review of Environment and Resources*, *37*, 107-136. https://doi.org/10.1146/annurev-environ-051112-111930

Chen, G. (2011). Theoretical efficiency of solar thermoelectric energy generators. *Journal of Applied Physics*, *109*(10), 104908. http://dx.doi.org/10.1063/1.3583182

Clark, W. (2015). *Sustainable Communities Design Handbook*. Elsevier Press, Germany.

Crane, D., Kossakovski, D., Bell, L., J. Electron. Mater. 38:1382-1386 (2009). Liu, D.; Jin, A.; The computer simulation with the finite elements method of triple stack TEPG predicts that the efficiency can achieve over 19%, HNCERI internal report, 2013.

Deng, Y. G., & Liu, J. (2009). Recent advances in direct solar thermal power generation. *Journal of Renewable and Sustainable Energy*, *1*(5), 052701. http://dx.doi.org/10.1063/1.3212675

Jin, A. J., & Zhang, Y. (2017). Systematic Studies on Building the High Output Thermoelectric Power Generation. International Journal of Science, Technology and Society, 5(4), 112-119.

Jin, A. J., Peng, W., Jin, Y., Liu, D., & Li, Q. (2013). Research, Development, and Applications of the High-Power Thermoelectric Generation Technology. *ARPN Journal of Science and Technology, 3*, 901.

Liu, D., & Jin, A. (2015). SW copyrights Reg.ID.: 2015SR094544 V1.0, China; 2015.

Liu, D., Li, Q., Peng, W., Zhu, L., Gao, H., Meng, Q., & Jin, A. J. (2015). Developing instrumentation to characterize thermoelectric generator modules. *Review of Scientific Instruments*, *86*(3), 034703.

Mao, J., Liu, Z., & Ren, Z. (2016). Size effect in thermoelectric materials. *npj Quantum Materials*, *1*, 16028. Retrieved from http://www.nature.com/articles/npjquantmats201628

Min, G., & Rowe, D. M. (2007). Conversion efficiency of thermoelectric combustion systems. *IEEE Transactions on energy Conversion*, *22*(2), 528-534.

Nolas, G. S., Sharp, J., & Goldsmid, J. (2013). *Thermoelectrics: basic principles and new materials developments* (Vol. 45). Springer Science & Business Media.

Solla, S. A. (1981). SA Solla and EK Riedel, Phys. Rev. B 23, 6008 (1981). *Phys. Rev. B*, *23*, 6008.

Thomson, W. (1857). 4. on a mechanical theory of thermo-electric currents. *Proceedings of the Royal society of Edinburgh*, *3*, 91-98.

Tritt, T. M., & Subramanian, M. A. (2006). Thermoelectric materials, phenomena, and applications: a bird's eye view. *MRS bulletin*, *31*(3), 188-198. http://dx.doi.org/10.1557/mrs2006.44

Ursell, T. S., & Snyder, G. J. (2002, August). Compatibility of segmented thermoelectric generators. In *Thermoelectrics, 2002. Proceedings ICT'02. Twenty-First International Conference on* (pp. 412-417). IEEE.

Yang, D., & Yin, H. (2011). Energy conversion efficiency of a novel hybrid solar system for photovoltaic, thermoelectric, and heat utilization. *IEEE Transactions on Energy Conversion*, *26*(2), 662-670.